

Synthesis and Characterization of Zinc Oxide Nanoparticles for Antibacterial Applications

S. Naseem Shah^{a,*}, S. Imran Ali^b, S. Rizwan Ali^a, M. Naeem^a, Yasmeen Bibi^c, S. Rehan Ali^a, S. Masood Raza^a, Yousuf Khan^d and Sikander Khan Sherwani^e

^aDepartment of Physics, Federal Urdu University of Arts, Sciences and Technology, Karachi, Pakistan

^bDepartment of Applied Chemistry and Chemical Technology, University of Karachi, Karachi, Pakistan

^cDepartment of Chemistry, Federal Urdu University of Arts, Sciences and Technology, Karachi, Pakistan

^dCentralized Science Laboratory, University of Karachi, Karachi, Pakistan

^eDepartment of Microbiology, Federal Urdu University of Arts, Sciences and Technology, Karachi, Pakistan

Abstract: ZnO nanoparticles are synthesized for antibacterial applications by a simple co-precipitation method. X-ray diffraction (XRD) reveals that the synthesized ZnO has hexagonal crystal structure with mean crystallite size of 29 nm. Scanning electron microscopy (SEM) and Energy dispersive x-ray spectroscopy (EDX) shows pure ZnO with uniform morphology. UV–VIS absorption spectroscopy yield an absorption edge in the range 300–400 nm which corresponds to a band gap energy of 3.50 eV. Antibacterial activity of ZnO nanoparticles is tested against gram positive and gram negative bacteria by using agar-well method. These ZnO nanoparticles are found to be strongly antimicrobial as they effectively prevent the growth of many test microorganisms with a small minimum inhibitory concentrations (MIC) ~ 80 – 280 µg/ml.

Keywords: Nanoparticles, Chemical synthesis, Zinc oxide, Optical property, Antibacterial activity.

INTRODUCTION

Outstanding optical absorption features of ZnO and its biocompatibility have resulted in many modern day cosmetic products employing ZnO nanoparticles as key ingredient [1,2]. These include lotions, ointments, medicated creams and sunscreens etc. In this context, the remarkable antimicrobial properties ZnO are also of relevance especially for medical and biological applications [3,4]. Additionally, due to successive use of antibiotics, microorganisms have developed immunity against them. This situation certainly demands new antibacterial compounds such ZnO based on advanced functional materials [5].

It has been shown that ZnO nanoparticles exhibit antimicrobial activity against a number of microorganisms [6,7]. To realize the full potential of ZnO as an antimicrobial agent, controlled and cost-effective synthesis of pure, uniform (monodisperse) and crystalline ZnO nanoparticles is of prime importance. A low-cost and simple synthesis with a high yield will guarantee successful commercialization of the product. Synthesis of nanoparticles via chemical methods has already been employed for producing advanced functional nanomaterials exhibiting better

semiconducting, optical and piezoelectric properties [3,8]. In particular, ZnO nanoparticles synthesized via chemical routes are found to be biologically compatible and environment friendly. Chemical synthesis usually involves ambient temperature thereby reducing the cost and complexity of the synthesis process. Many chemical routes to synthesized ZnO have been reported in literature such as sol–gel [9], thermal decomposition [10], micro emulsion [11] etc. However, all these methods either involve a number of unwanted chemicals or complex process steps. Thus the purity and yield of the sample always remain an issue.

Here, we present a simple co-precipitation method to synthesize uniform, spherically shaped and pure ZnO nanoparticles using zinc acetate as a metal precursor and dimethylformamide as a precipitating agent. No other dispersing or structure directing agents are used. X-ray diffraction shows that the synthesized ZnO nanoparticles have hexagonal crystal structure with an average crystallite size of 29 nm. Scanning electron microscopy (SEM) reveals that the as synthesized nanoparticles acquire uniform morphology. Energy dispersive x-ray spectroscopy (EDX) confirms that the synthesis process yields pure ZnO nanoparticles within its detection limit. UV–VIS absorption spectroscopy yield an absorption edge value for ZnO nanoparticles in the wavelength ranges of 300–400 nm. The band gap energy of the sample is found to be 3.50 eV, which is larger than the one

*Address correspondence to this author at the Department of Physics, Federal Urdu University, Gulshan-e-Iqbal Campus Block 9, Karachi, Pakistan;
E-mail: syednaseemshah@fuuast.edu.pk

reported for bulk samples (3.20 eV) [12]. The antibacterial activity of ZnO nanoparticles is systematically tested against gram positive (G^+) bacteria and gram negative (G^-) bacteria by using agar-well method. The results show that ZnO nanoparticles are strongly antimicrobial as they successfully suppressed the growth of a number of test microorganisms.

EXPERIMENTAL DETAILS

The co-precipitation operations commonly contain the substances like hydroxide, carbonates, sulphates, acetates and oxalates [13]. In this particular research, we adopt the co-precipitation method for the preparation of nanoparticles of ZnO of nearly uniform size [14]. Zinc acetate dehydrate and DMF were used for synthesizing ZnO nanoparticles and all chemical were purchased from *Merck* and are of analytical grade. All the glassware were cleaned first with distilled water and then with acetone and dry air. The desired amount of Zinc acetate dehydrate was weighted on an electronic balance and mixed with 200 ml of DMF in a round bottom flask. The mixture was stirring at room temperature for 30 minutes to make a homogeneous mixture. Thereafter, the temperature of the flask was raised to and kept stable at 200 °C for 3 hours on a hot plate with continuous stirring. The mixture was then brought to room temperature (RT) and wash several

time to remove unreacted product. After that the obtained yield of the sample was centrifuged at 4000 rpm to separate the precipitates. The resulting sample was dried at 70 °C in an oven for 24 hours and then annealed at 400 °C for 10 hours.

RESULTS AND DISCUSSION

X-ray diffraction (XRD) was performed on ZnO nanoparticles to determine the particle size and phase purity. We use a Bruker Axis, D8 Advance diffractometer with Cu K_α radiation ($\lambda = 1.54 \text{ \AA}$) at 40 kV. Figure 1 shows the XRD pattern of ZnO nanoparticles. The XRD peaks are significantly broader as compared to bulk samples [15]. Briefly, a peak in the diffraction pattern originates from the sum of the diffracted intensities over all atoms in the crystal [16]. Due to the large number of atoms in bulk crystals the sum generally converge resulting in a delta function or a very narrow peak. Nanoparticles on the other hand consists of small crystallites having finite number of atoms. Thus the diffracted intensity does not converge effectively and a rather broad peak results. The data obtained from X-rays diffractometer are further refined using Maud material analysis software. XRD pattern of the sample has prominent peaks at 2 theta values of 31.73°, 34.37°, 36.21°, 47.47°, 56.55°, 62.77°, 66.31°, 67.87° and 69.01° corresponding to (100), (002), (101), (102), (110), (103), (200), (112) and (201) planes. The

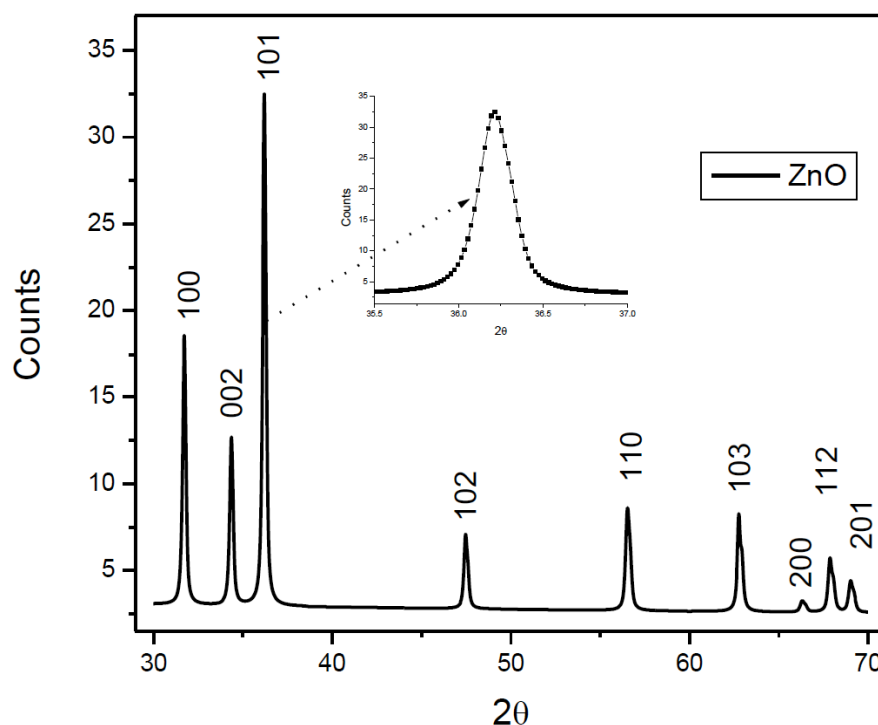


Figure 1: XRD pattern of ZnO nanoparticles. Inset shows magnified view of (101) peak.

lattice constants of our sample are found to be $a=b=3.2530 \text{ \AA}$ and $c = 5.2130 \text{ \AA}$ in good agreement with the values of hexagonal ZnO of the space group P63mc. The (hkl) values are also in good agreement with the standard card of ZnO powder [17].

The average size of nanoparticles is found by using Debye-Scherrer equation.

$$D=0.9\lambda/\beta\text{Cos } \theta$$

where, λ , β and θ are the X-ray wavelength of (Cu-K α), the full width at half maximum and the angle of (101) diffraction plane respectively. The crystallite size of the sample is found to be around 29 nm. The SEM image of ZnO nanoparticles is shown in Figure 2. A high degree of agglomeration is clearly visible in agreement with previous studies [18]. The observation of some larger nanoparticles in SEM image is attributed to agglomeration [19]. EDX spectrum of ZnO nanoparticle samples is shown in Figure 3. The names and percentages of the elements for the ZnO sample are shown in the labeling. Clearly, Zn and O are the main constituents of the sample [20] and no trace of impurities could be found within the detection limit of EDX.

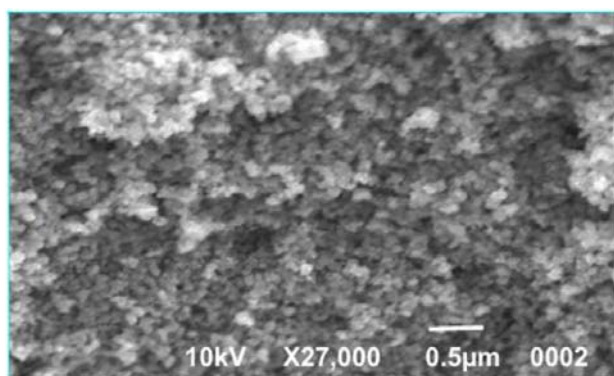


Figure 2: Morphology of Zinc Oxide Nanoparticles.

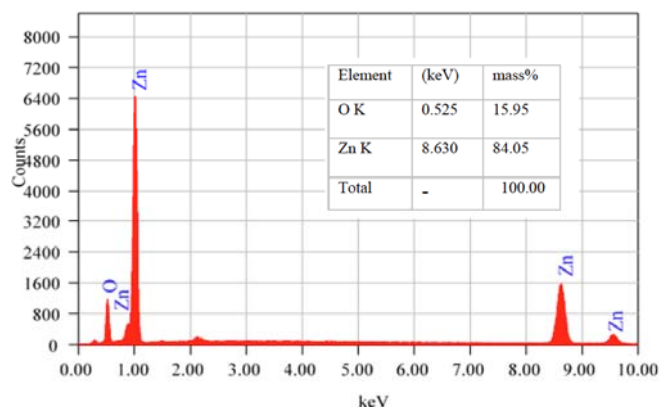


Figure 3: EDX Spectra of Zinc Oxide Nanoparticles.

Optical properties of the samples were studied by UV–VIS absorption spectroscopy. The absorption spectra of sample were recorded in the range 300 nm to 900 nm by a UV-2600 Spectrometer (Shimadzu). We use DMF as the reference solution for the absorption spectrum of ZnO nanoparticles. Figure 4 shows the UV-VIS spectrum for ZnO nanoparticle. It should be noted that the absorption edge values for ZnO samples lie in the wavelength ranges of 300 - 400 nm. The observed UV peak is found to be in good agreement with previously reported [21] free exciton transition peak. This transition is an intrinsic feature of the wurtzite ZnO and has its origin in the excitonic recombination [22].

The type of electronic transition and band gap can be determined with the help of optical absorption spectrum. When the band gap (E_g) of a semiconductor is smaller than the photons of higher energy, an electron is transferred from the valence band to the conduction band. This causes an abrupt increase in the absorbency of the material to the wavelength corresponding to the band gap energy [23]. The relation of the absorption coefficient (α), incident photon energy $h\nu$ and E_g is given by,

$$\alpha = (h\nu - E_g)^{\frac{1}{2}} \frac{A}{h\nu}$$

where $h\nu$ photon energy, $\alpha = 4\pi k / \lambda =$ absorption coefficient ($k =$ absorption index or absorbance) and $A =$ constant. The value of E_g is found to be around 3.50 eV by the straight line portion of $(\alpha h\nu)^2 = 0$ axis; (see Figure 5). The value of E_g is found to be larger than the bulk value in agreement with Ref. [9]. A shift in the E_g of ZnO nanoparticles from its bulk value of 3.20 eV is observed [24]. The increase in the E_g with decrease in the crystallite size is due to finite size effects.

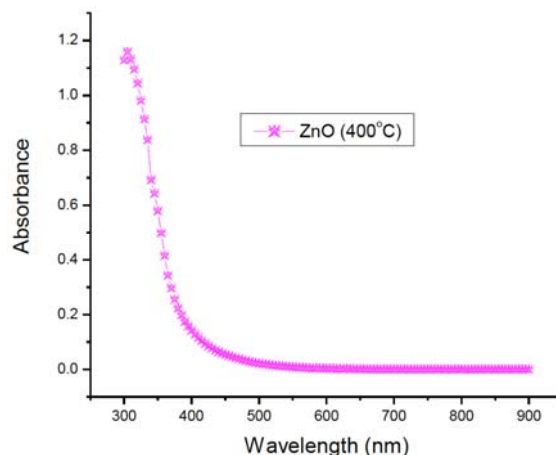


Figure 4: UV-VIS spectra of ZnO Nanoparticles.

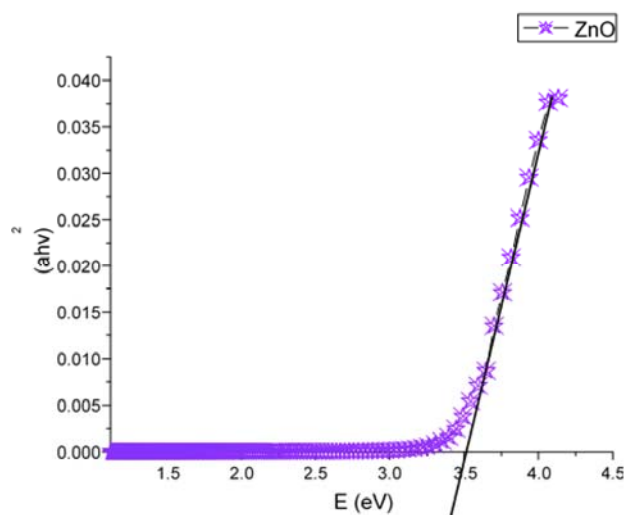


Figure 5: $(\alpha hv)^2$ vs. photon energy (hv) of ZnO nanoparticles.

Furthermore, we have tested the antimicrobial activity of our ZnO nanoparticles against thirteen G^+ bacteria and twenty G^- bacteria. Muller Hinton Agar and Muller Hinton Broth were used as culturing media for bacterial strains according to the procedure described in Ref. [25]. ZnO nanoparticles were then tested for their antibacterial activity against thirteen G^+ bacteria and twenty G^- bacteria, by using Agar-well method. Initially, the bacterial culture was refreshed using autoclaved Muller Hinton broth. Thereafter, wells of suitable size and separation were punched into Muller Hinton Agar and 10 micro-liters of bacteria culture was carefully dispensed into the wells [26]. The plates were then allowed to incubate at 28 °C for 1 to two days after which the incubation diameter of zone of inhibition (ZI) was noted by Vernier caliper. Table 1 shows the estimated values ZI for different bacteria. As a standard antibiotic Gentamicin was used. It should be noted that out of 13 G^+ and 20 G^- bacteria, ZnO nanoparticles exhibit significant antibacterial features against 4 G^+ and 6 G^- bacteria. No antibacterial activity could be noticed for the rest of the bacteria studied. For G^+ bacteria, ZnO exhibits maximum activity (22±2) against *Bacillus subtilis* and minimum activity ((13±2) against *Bacillus cereus* bacteria. On the other hand for G^- bacteria, the maximum (20±1) and minimum (10±0) activities were recorded for *Enterobacter aerogenes* and *E. coli*, respectively.

Beside the size of inhibition zone, Minimum inhibitory Concentration (MIC) of ZnO sample can also be used to quantify its antibacterial activity. MIC is the minimum concentration of antibacterial agent that stops visible growth of bacteria after overnight exposure. Clearly, a small value of MIC means strong

antibacterial activity. In order to estimate the MIC of the sample by Micro broth dilution method using 96-well microtiter plate [27] the following steps were performed. *Step-1:* Solution-A of the nanoparticles was prepared in ultra-pure distilled water for a range of concentrations 10 µg/ml – 1 µg/ml. *Step-2:* Microbial inoculums were prepared in microtiter plate by sub culturing microorganisms (at 37 °C for 2 hrs) into standard Muller Hinton Broth (MHB) [28]. These were diluted to approximately 10⁵ to 10⁶ of organisms/ml in MHB (Solution-B). *Step-3:* A 100 µl of solution A (for each dilution) is added to 100 µl of solution B (for each test microorganism) in the microplate wells [29]. *Step-4:* These plates were incubated at 37 °C for one day. Thereafter, 40 µL, 0.02 mg/ml triphenyl tetrazolium chloride (TTC) were poured in each microplate well. This caused in a change of color of TTC from colorless to red due to microbial growth [30]. *Step-5:* Finally, the MIC of ZnO nanoparticles was determined as the lowest concentration that stopped the visible growth of the test microorganism.

The estimated values of MICs against different bacteria mentioned Table 1, are presented in Table 2. The antibacterial activity of ZnO nanoparticles were determined against thirteen G^+ bacteria (*Bacillus(B) cereus*, *Bacillus(B) subtilis*, *Bacillus(B) thuringiensis*, *Corynebacterium(C) diphtheriae*, *Corynebacterium(C) hofmannii*, *Corynebacterium(C) xerosis*, *Staphylococcus(S) epidermidis*, *Streptococcus(S) saprophyticus*, *Staphylococcus(S) aureus*, *Staphylococcus(S) aureus AB 188*, *M. smegmatis*, *Streptococcus(S) fecalis*, *Streptococcus(S) pyogenes*). The result showed that only 4 gram positive bacteria were found active for ZnO nanoparticles as shown in Table 1. The twenty G^- bacteria were screened (*Enterobacter(E) aerogenes*, *Escherichia(E) coli ATCC 8739*, *Escherichia(E) coli*, *E. coli multi drug resistance*, *Klebsiella (K) pneumonia*, *Salmonella(S) typhi*, *Salmonella(S) paratyphi A*, *Salmonella(S) paratyphi B*, *Shigella(S) dysenteriae*, *Serratia(S) marcescens*, *Acinetobacter(A) baumannii*, *Campylobacter(C) jejuni*, *Campylobacter(C) coli*, *Helicobacter(H) pylori*, *Hemophilus(H) influenza*, *Vibrio(V) cholera*, *Aeromonas(A) hydrophila*, *Proteus(P) mirabilis*, *Pseudomonas(P) aeruginosa* and *Pseudomonasaeruginosa ATCC*). Among these gram negative bacteria 6 bacteria were found active for the sample as shown in Table 2.

CONCLUSION

ZnO nanoparticles are synthesized and tested for their antibacterial activity against thirteen gram

Table 1: Antibacterial Potential of ZnO Nanoparticles

Gram positive bacteria	Zone of inhibition in mm (mean \pm S.D)	Gram negative bacteria	Zone of inhibition in mm (mean \pm S.D)
<i>Bacillus cereus</i>	13 \pm 2	<i>Enterobacter aerogenes</i>	20 \pm 1
<i>Bacillus subtilis</i>	22 \pm 2	<i>Escherichia coli</i> ATCC 8739	12 \pm 1
<i>Bacillus thuringiensis</i>	20 \pm 1	<i>Escherichia coli</i>	10 \pm 2
<i>Staphylococcus epidermidis</i>	15 \pm 1	<i>E. coli</i> multi drug resistance	10 \pm 0
-	-	<i>Serratia marcesens</i>	10 \pm 1
		<i>Acinetobacter baumannii</i>	18 \pm 0

Table 2: Minimum Inhibitory Concentration of ZnO Nanoparticles

Gram positive bacteria	Minimum inhibitory concentration (μ g/ml)	Gram negative bacteria	Minimum inhibitory concentration (μ g/ml)
<i>Bacillus cereus</i>	260	<i>Enterobacter aerogenes</i>	80
<i>Bacillus subtilis</i>	280	<i>Escherichia coli</i> ATCC 8739	100
<i>Bacillus thuringiensis</i>	140	<i>Escherichia coli</i>	180
<i>Staphylococcus epidermidis</i>	120	<i>E. coli</i> multi drug resistance	180
-	-	<i>Serratia marcesens</i>	120
-	-	<i>Acinetobacter baumannii</i>	180

positive bacteria and twenty grams negative bacteria by using agar-well method. These ZnO nanoparticles are synthesized by a simple co-precipitation method. X-ray diffraction confirms the formation of hexagonal ZnO nanoparticles with lattice constants $a=b= 3.2530 \text{ \AA}$ and $c = 5.2130 \text{ \AA}$. The average crystallite size of is found to be 29 nm using Debye-Scherrer formula. Scanning electron microscopy (SEM) reveals that as synthesized nanoparticles are monodisperse. No trace of impurity could be detected by Energy dispersive x-ray spectroscopy (EDX). UV-VIS absorption spectroscopy yield an absorption edge value in the wavelength ranges of 300-400 nm and a band gap of 3.50 eV. The ZnO nanoparticles are found to exhibit strong antimicrobial features with quite low values of minimum inhibitory concentrations (MIC) ~ 80 – 280 μ g/ml.

ACKNOWLEDGEMENT

The work at Nanoscale Condensed matter research Laboratory (NCRL), Department of Physics Federal Urdu University, Karachi is partially supported by FUUAST Dean research grant titled "Mini-project 2016"

REFERENCES

- [1] Applerot G, Lellouche J, Perkas N, Nitzan Y, Gedanken A, Banin E. ZnO nanoparticle-coated surfaces inhibit bacterial biofilm formation and increase antibiotic susceptibility. *RSC Adv* 2012; 2: 2314-2321. <http://dx.doi.org/10.1039/C2RA00602B>
- [2] Yu SF, Yuen C, Lau SP, Park WI, Yi GC. Random laser action in ZnO nanorod arrays embedded in ZnO epilayers. *Appl Phys Lett* 2004; 84: 3241-3243. <http://dx.doi.org/10.1063/1.1734681>
- [3] Peter KS, Rosalyn LK, George LM, Kenneth JK. Metal oxide nanoparticles as bactericidal agents. *Langmuir* 2002; 18: 6679-6686. <http://dx.doi.org/10.1021/la0202374>
- [4] Premanathan M, Karthikeyan K, Jeyasubramanian K, Manivannan G. Selective toxicity of ZnO nanoparticles toward Gram-positive bacteria and cancer cells by apoptosis through lipid peroxidation. *Nanomed Nanotechnol. Biol Med* 2011; 7: 184-192. <http://dx.doi.org/10.1016/j.nano.2010.10.001>
- [5] Xie Y, He Y, Irwin PL, Jin T, Shi X. Antibacterial activity and mechanism of action of zinc oxide nanoparticles against *Campylobacter jejuni*. *Appl Environ Microbiol* 2011; 77: 2325-2331. <http://dx.doi.org/10.1128/AEM.02149-10>
- [6] Huang Z, Zheng X, Yan D, Yin G, Liao X, Kang Y, Yao Y, Huang D, Hao B. Toxicological effect of ZnO nanoparticles based on bacteria. *Langmuir* 2008; 24: 4140-4144. <http://dx.doi.org/10.1021/la7035949>
- [7] Sawai J, Yoshikawa T. Quantitative evaluation of antifungal activity of metallic oxide powders (MgO, CaO and ZnO) by an indirect conductimetric assay. *Journal of Applied Microbiology* 2004; 96: 803-809. <http://dx.doi.org/10.1111/j.1365-2672.2004.02234.x>
- [8] Huang MH, Mao S, Feick H, Yan H, Wu Y, Kind H, Weber E, Russo R, Yang P. Room-temperature ultraviolet nanowire nanolasers. *Science* 2001; 292(5523): 1897-1899. <http://dx.doi.org/10.1126/science.1060367>

[1] Applerot G, Lellouche J, Perkas N, Nitzan Y, Gedanken A, Banin E. ZnO nanoparticle-coated surfaces inhibit bacterial

- [9] Seema R, Poonam S, Shishodia, Mehra RM. Synthesis of nanocrystalline ZnO powder via sol-gel route for dye-sensitized solar cells. *Solar Energy Materials & Solar Cells* 2008; 92: 1639-1645. <http://dx.doi.org/10.1016/j.solmat.2008.07.015>
- [10] Svetozar M, Ankica S, Stanko P. Formation of nanosize ZnO particles by thermal decomposition of zinc acetylacetonate monohydrate. *Ceramics International* 2010; 36(3): 1117-1123. <http://dx.doi.org/10.1016/j.ceramint.2009.12.008>
- [11] Agrell J, Germani G, Jaras SG, Boutonnet M. Production of hydrogen by partial oxidation of methanol over ZnO-supported palladium catalysts prepared by microemulsion technique. *Appl Catal A* 2003; 242: 233-245. [http://dx.doi.org/10.1016/S0926-860X\(02\)00517-3](http://dx.doi.org/10.1016/S0926-860X(02)00517-3)
- [12] Singh S, Chakrabarti P. Comparison of the structural and optical properties of ZnO thin films deposited by three different methods for optoelectronic applications, *Superlattices Microstruct* 2013; 64: 283-293. <http://dx.doi.org/10.1016/j.spmi.2013.09.031>
- [13] Noboru I, Ozaki Y, Kashu S, James M. Superfine particle technology. New York: Springer Verlag; 1992. Available from: <http://link.springer.com/book/10.1007/978-1-4471-1808-4>
- [14] Kumar S, Asokan K, Kumar SR, Chatterjee S, Kanjilal D, Kumar GA. Investigations on structural and optical properties of ZnO and ZnO:Co nanoparticles under dense electronic excitations. *RSC Adv* 2014; 4: 62123-62131. <http://dx.doi.org/10.1039/C4RA09937K>
- [15] Jian MZ, Yan Z, Ke-Wei X, Vincent J. General compliance transformation relation and applications for anisotropic hexagonal metals. *Solid State Communications* 2006; 139: 87-91. <http://dx.doi.org/10.1016/j.ssc.2006.05.026>
- [16] Tamus U. The Meaning of Size Obtained from Broadened X-ray Diffraction Peaks. *Advanced Engineering Materials* 2003; 5: 323-329. <http://dx.doi.org/10.1002/adem.200310086>
- [17] Powder Diffraction File, Alphabetical Index, Inorganic Compounds, Published by JCPDS International Centre for Diffraction Data, Newtown Square, PA. 19073, 2003 (JCPDS Card No.: 36-1451).
- [18] Chou TP, Qifeng Z, Glen EF, Guozhong C. Hierarchically Structured ZnO Film for Dye-Sensitized Solar Cells with Enhanced Energy Conversion Efficiency. *Adv Mater* 2007; 19: 2588-2592. <http://dx.doi.org/10.1002/adma.200602927>
- [19] Caglara M, Yakuphanoglu F. Structural and optical properties of copper doped ZnO films derived by sol-gel. *Applied Surface Science* 2012; 258: 3039-3044. <http://dx.doi.org/10.1016/j.apsusc.2011.11.033>
- [20] Rana SB, Singh P, Sharma AK, Carbonari AW, Dogra R. Synthesis and characterization of pure and doped ZnO nanoparticles. *Journal of Optoelectronics and Advanced Materials* 2010; 12: 257-261. <https://www.ipen.br/biblioteca/2010/16402.pdf>
- [21] Van Dijken A, Makkinje J, Meijerink A. The influence of particle size on the luminescence quantum efficiency of nanocrystalline ZnO particles. *Journal of Luminescence*. 2001; 92(4): 323-328. [http://dx.doi.org/10.1016/S0022-2313\(00\)00262-3](http://dx.doi.org/10.1016/S0022-2313(00)00262-3)
- [22] Naeem M, Qaseem S, Gul I, Maqsood A. Study of active surface defects in Ti doped ZnO nanoparticles. *J Appl Phys* 2010; 107: 124303. <http://dx.doi.org/10.1063/1.3432571>
- [23] Wang JF, Wen BS, Hong C, Wen XW, Guo Z. (Pr, Co, Nb)-Doped SnO₂ Varistor. *J Am Ceram Soc* 2005; 88: 331-334. <http://dx.doi.org/10.1111/j.1551-2916.2005.00095.x>
- [24] Viswanatha R, Sapra S, Satpati B, Satyam PV, Dev BN, Sarma DD. Understanding the quantum size effects in ZnO nanocrystals. *Journal of Materials Chemistry* 2004; 14:661-668. <http://dx.doi.org/10.1039/b310404d>
- [25] Talat M, Yasmeen B, Humera I, Iffat M, Aneela W, Sikandar S. Complexation and Antimicrobial activities of β sitosterol with trace metals. (Cu (II), Co (II), and Fe (III)). *European Academic Research* 2013; 1: 677-685. Available from: <http://euacademic.org/UploadArticle/100.pdf>
- [26] Perez C, Paul M, Bazerque P. An antibiotic assay by the agar well diffusion method. *Acta Biol Med Exp* 2009; 15: 113-115.
- [27] Julia AK, George EH, Max S, Wendy A, Catherine M, Cynthia C. Use of the National Committee for Clinical Laboratory Standards Guidelines for Disk Diffusion Susceptibility Testing in New York State Laboratories. *J Clin Microbiol* 2000; 38(9): 3341-3348. Available from: <http://www.ncbi.nlm.nih.gov/pmc/articles/PMC87384/>
- [28] Olson CR, Balasubramaniam T, Shrum J, Nord T, Taylor PL, Burrell RE. Novel Antimicrobial Activity of Nanocrystalline Silver Dressings. *Int. Congress on MEMS* 2005; 129-131. <http://dx.doi.org/10.1109/ICMENS.2005.90>
- [29] Sougata S, Atish DJ, Samir KS, Golam M. Facile synthesis of silver nano particles with highly efficient anti-microbial property. *J Polyhedron* 2007; 26: 4419-4426. <http://dx.doi.org/10.1016/j.poly.2007.05.056>
- [30] Navarro V, Villarreal ML, Rojas G, Lozoya X. Antimicrobial evaluation of some plants used in Mexican traditional medicine for the treatment of infectious diseases. *J Ethnopharmacol* 1996; 53(3): 143-147. [http://dx.doi.org/10.1016/0378-8741\(96\)01429-8](http://dx.doi.org/10.1016/0378-8741(96)01429-8)

Received on 21-03-2016

Accepted on 12-04-2016

Published on 29-04-2016

<http://dx.doi.org/10.6000/1927-5129.2016.12.31>

© 2016 Shah et al.; Licensee Lifescience Global.

This is an open access article licensed under the terms of the Creative Commons Attribution Non-Commercial License (<http://creativecommons.org/licenses/by-nc/3.0/>) which permits unrestricted, non-commercial use, distribution and reproduction in any medium, provided the work is properly cited.